Energy, Mines and Resources Canada | Énergie, Mines et Ressources Canada

CANMET

Canada Centre for Mineral and Energy Technology | Centre canadien de la technologie des minéraux et de l'énergie

DEGRADATION OF DIRECT BONDED CHROME MAGNESIA BRICKS IN SECONDARY STEELMAKING UNDER VACUUM

D.H.H. Quon and K.E. Bell
Mineral Processing Laboratory

February 1983

Project MRP-3.6.0.0.72
Electrodes and Refractories for the Steel Industry

This document is an unedited interim report prepared primarily for discussion and internal reporting purposes. It does not represent a final expression of the opinion of the Canada Centre for Mineral and Energy Technology (CANMET)

Ce document est un rapport provisoire non-révisé et rédigé principalement pour fin de discussion et de documentation interne. Il ne représente nullement l'expression définitive de l'opinion du Centre canadien de la technologie des minéraux et de l'énergie (CANMET)

34pp

MINERALS RESEARCH PROGRAM
MINERAL SCIENCES LABORATORIES
DIVISION REPORT MRP/MSL 83-7 (IR)

DEGRADATION OF DIRECT BONDED CHROME MAGNESIA BRICKS IN SECONDARY STEELMAKING UNDER VACUUM

by

D.H.H. Quon* and K.E. Bell**

ABSTRACT

Failure of direct bonded chrome magnesia bricks from steelmaking ladles was examined in terms of structural characteristics and chemical changes. Refractories degradation is in part caused by slag infiltration along the grain boundaries of the periclase and spinel. Other factors that cause the failure of refractories are the presence of intergranular phases such as Ca and Si and the loss of magnesium oxide under vacuum at high temperature. All these factors have a great influence in determining the strength of the refractories under operating conditions.

---

*Research Scientist and ** Head, Ceramic Section, Mineral Processing Laboratory, Mineral Sciences Laboratories, CANMET, Energy, Mines and Resources Canada, Ottawa.

CONTENTS

	Page
ABSTRACT	1
INTRODUCTION	1
CLASSIFICATION OF REFRACTORIES	1
EXPERIMENTAL PROCEDURE	2
Materials	2
Characterization	3
Cup Tests	3
RESULTS	3
Microscopy	4
Degradation of Refractories at Low Pressure and High Temperature	5
Slag Corrosion Tests	6
Thermal Shock and Expansion Behaviour	7
Porosity and Density of Used and Unused Bricks	7
DISCUSSION	8
CONCLUSIONS	8
ACKNOWLEDGEMENTS	9
REFERENCES	10

TABLES

No.		
1.	Chemical compositions of slags used for the cup tests	12
2.	Density and porosity of the chrome bricks	13

FIGURES

No.		
1.	Typical microstructure of an unused brick	14
2.	Photomicrograph showing exsolved spinel phase in and around the periclase grains	14
3.	Micrograph showing coarse grained periclase containing finely exsolved spinel phase	15
4.	Micrograph showing coarse grained chrome spinel crystals in a periclase matrix	15

No.		Page
5.	The skeletal crystals of spinel in a periclase matrix	16
6.	SEM micrograph of an unused brick	16
7.	EDXR map of Ca of an unused brick	17
8.	EDXR map of Si of an unused brick	17
9.	EDXR map of Fe of an unused brick	18
10.	Microstructure of a used brick at the slag brick interface	18
11.	Microstructure of a used brick viewed under transmitted light ..	19
12.	Microstructure of a used brick showing highly slag resistant spinel phase in a groundmass of slag	19
13.	Microstructure of a used brick showing partial penetration by the slag	20
14.	Micrograph showing slag penetration in the grog grain of periclase and disruption of solid-solid bond of the grains	20
15.	SEM micrograph of a slagged brick used above the slagline	21
16.	EDXR map of Mg of a slagged brick	21
17.	EDXR map of Ca of a slagged brick	22
18.	EDXR map OF Si of a slagged brick	22
19.	Vapourization loss versus duration of heating at 1700°C of an unused brick	23
20.	Photograph showing direct bonded brick prior to firing (left) and after firing at 1700°C for 5 hours (right)	23
21.	SEM micrograph of the surface of a brick after firing, higher magnification	24
22.	SEM micrograph of the surface of a brick after firing	24
23.	SEM micrograph of a fracture surface of an unused brick	25
24.	SEM micrograph of the fracture surface of a used brick at about 8 cm behind the slag brick interface	25
25.	SEM micrograph of the fracture surface of a slag infiltrated brick	26
26.	Section through crucible after slag infiltration	26
27.	Micrograph showing lath-shaped silicates formed in slagged brick	27
28.	SEM micrograph showing dissolution or periclase grains by slag	27

Page

29. EDXR map of Ca of a slag-corroded crucible 28
30. EDXR map of Si of a slag-corroded crucible 28
31. EDXR map of Al of a slag-corroded crucible 29
32. EDXR map of Fe of a slag-corroded crucible 29

INTRODUCTION

Various vacuum processes developed in the past decade for different metallurgical objectives have created a need for low wear, high quality refractories for use in steelmaking ladles. Refractory wear can be of decisive importance for the economy of the process, and therefore it is important that the wear behaviour in practice and in the laboratory be examined with the aim of reducing the wear rate. Also it is essential that the most suitable refractories are selected for any particular application. The most serious refractory failure has been ascribed to a combination of chemical attack and mechanical erosion where the refractories were in contact with slag and molten steel as well as to thermal shock due to drastic temperature changes (1-11). Recently, attempts have been made to correlate refractory failure with the rate of loss of oxide constituents at high temperature and low pressure (12-18).

A more recent study made in CANMET, involving the co-clinkered chrome-magnesia bricks used in secondary steelmaking under vacuum environment, showed that the failure of the refractories is in part caused by slag infiltration (13). A particularly significant finding was that at high temperature and low pressure, a substantial loss of MgO occurred and this in turn caused the weakening of the bond between the chrome spinel and periclase grains.

The aim of the present study is to examine the direct bonded chrome-magnesia bricks which are also used in the ladles. This study forms part of a program to examine the failure of basic refractories in vacuum refining processes, which has been identified by the Canadian Steel and Iron Research Association (CSIRA) as a serious problem encountered commercially.

CLASSIFICATION OF REFRACTORIES

A wide variety of chrome-magnesia refractories are available commercially for high temperature application. The five distinctive classes of chrome-magnesia refractories are:

a) Conventional chrome-magnesia brick,

b) Direct bonded chrome-magnesia brick,

c) Simultaneous sinter chrome-magnesia brick,

d) Fused grain or co-clinkered chrome-magnesia brick,

e) Fusion cast chrome-magnesia brick.

Basically, all these bricks are made up of chrome spinel and periclase grains. However, the distribution of these phases differs in them and the degree of solid solution and exsolution of these phases also vary. All these variations result from the different fabrication techniques. Both fused grain or co-clinker and direct bonded bricks are used most extensively in secondary steelmaking for lining the ladles. The co-clinkered brick is superior in slag resistance as this material is fabricated by mixing finely divided chromite concentrates with magnesia powder. The mixture after pelletizing is sintered by firing in rotary kiln, at high temperture. This process produces a homogeneous distribution of the spinel phase in the material. Other beneficial effects of this process include properties such as low silicate content and high resistance to dissolution when in contact with slag and hence this material is normally used in a more critical area in the ladle. The direct bonded brick is normally composed of relatively coarse chrome ore and fine magnesia, and the term "direct bonded" describes the direct bonding of the magnesia and chrome spinel without an interrupting film or phase of silicate at the grain boundaries. The microstructural development of the brick is also controlled by firing. A progressive solid solution of chrome in periclase occurs as the firing temperature increases. Traditionally, the direct-bonded bricks are used in the low wear area in the ladle such as the lining above and below the slag line as dictated by the economical point of view.

Although, a considerable effort has been made in the past decade in improving the basic refractories, still the nature of refractory degradation under different operating conditions is not fully understood.

EXPERIMENTAL PROCEDURE

MATERIALS

The direct bonded chrome-magnesia bricks for this study were supplied by the Atlas Steel Company, Welland, Ontario.

CHARACTERIZATION

Both the used and unused bricks were first examined megascopically. Thin sections and/or polished sections of selected samples were made for microscopic examination. Scanning electron microscopy (SEM) was used to examine the microstructures that were not resolvable by optical microscopy. The energy dispersive X-ray (EDXR) technique was used to examine the distribution of various elements in the used and unused bricks.

CUP TESTS

The stability of the brick in contact with slag was examined. In this test, unused bricks were machined into small cylindrical blocks of approximately 30 mm in diameter by 35 mm high. A hole of 14 mm diameter by 30 mm depth was drilled at the centre of the small block, and was subsequently packed with ground slag. The cup was then loaded into a molybdenum safety crucible and then placed inside a graphite resistance furnace operated in vacuum at about 1700°C.

The compositions of the slags used for the cup tests are given in Table 1. These slags were also supplied by the Atlas Steel Company and had calcia to silica mass ratios ranging from 0.92 to 1.44.

Thermal shock behaviour of the used and unused bricks was determined by inserting 47 x 47 x 110 mm samples on end into a preheated furnace at 1000°C and air quenching to room temperature.

Thermal expansion of the used and unused bricks was determined by dilatometer to examine whether thermal expansion might have led to extra stressing along the slag infiltrated interface. The thermal expansion of the used and unused bricks were compared.

Both density and apparent porosity of the used and unused bricks were determined.

RESULTS

Megascopicaly, the colouration of the used and unused bricks is identical, showing light brown grog grains of periclase in a dark brown ground mass of chrome spinel and periclase.

Fractures were observed in the used brick and they were mainly parallel to the slag and brick interface.

MICROSCOPY

Typical microstructures of the unused brick are shown in Fig. 1 to 5. The dominant phases are periclase, as large grains, and chrome spinel. The latter occurs as euhedral or subhedral crystals randomly distributed in the periclase groundmass (Fig. 4, 5) and/or as variable amounts of an exsolved phase mainly within the periclase grains (Fig. 2, 3). Occasionally chrome spinel tends to rim the periclase grains at the grain boundaries, but this is uncommon. This is in contrast to the rebonded fused-grain brick in which such texture is very common (13).

A typical SEM micrograph of the unused brick is shown is Fig. 6. brick is shown in Fig. 6. Quantitative analysis of the sample using EDXR technique revealed that the Ca and Si impurities occurred at the grain boundaries of the periclase whereas the Fe appeared to concentrate in the spinel and the periclase grains. Elemental distribution maps for Ca, Si and Fe are given Fig. 7 to 9 respectively.

Microstructures of the used brick at a zone of slag and brick interface are given in the photomicrographs in Fig. 10 and 11. The polished section in Fig. 10 shows that the slag penetrated along a fracture of the brick and that lath-shaped silicate crystals replaced the periclase grains. Examination of the same area in thin section (Fig. 11) revealed that the silicate crystals are birefringent. The silicate crystal is monticellite as identified by the X-ray diffraction. The rounded grains of the periclase and the islands of undissolved exsolved blebs and euhedral crystals of the spinel phase indicate that the periclase dissolved and the chrome spinel remained intact during the slag infiltration.

Used bricks from both above and below the slag line have very similar microstructures at the slagbrick interface. One of the characteristic features common to these bricks is the chrome spinel pseudomorph of the periclase outlining the ghost periclase grains, which were in part replaced by the silicate (Fig. 12). Typical example areas that are relatively free from slag corrosion can be seen in Fig. 13, in which the spinel crystals are relatively fresh without significant alteration. The penetration of slag into the brick can also disrupt the solid-solid bond of the periclase crystals. A typical example of this is shown in Fig. 14. In this case the slag migrated along the grain boundaries of a large grog periclase grain.

The SEM micrograph in Fig. 15 shows the microstructure of a used brick at a zone near the slag and brick interface. The microstructure of this zone is identical to that observed under the optical microscope. Essentially, it shows euhedral grains of chrome spinel filled interstitially by lath shaped silicate crystals. EDXR maps for Mg, Ca and Si for this zone are given in Fig. 16 to 18 respectively. The results show that the chrome spinel crystals are enriched in Mg and the silicate phase is outlined by the distribution of Ca and Si.

DEGRADATION OF REFRACTORIES AT LOW PRESSURE AND HIGH TEMPERATURE

The volatilization loss of oxide constitutents from the co-clinkered chrome-magnesia refractories was discussed by Quon and Bell (13). A similar observation was reported by Orlov and his co-workers (15, 16).

The effect of high temperatures and low pressures on direct bonded chrome-magnesia brick was examined in this case. Small cubes, about 1.4 x 1.4 x 0.6 mm, were cut from the unused brick. A specimen was placed in a molybdenum crucible and then loaded into a graphite furnace. After the pressure of the furnace chamber was reduced to 0.13 Pa, the furnace temperature was raised to about 1700°C and the sample kept in the heated furnace for a period varying from 30 minutes to 5 hours. On completion of the heating cycle, the sample was removed from the furnace, and the weight change resulting from the heat treatment was obtained. The weight loss versus duration of heating of a series of samples is graphically presented in Fig. 19. The results show that the weight loss increases almost linearly with increasing soak time. Megascopic and microscopic inspection of the heat treated samples all show varying degrees of surface degradation and the refractories are loosely bonded together (Fig. 20). SEM micrographs of the degraded surface are given in Fig. 21 and 22. The characteristic morphology of the surface under high magnification shows that the spinel crystals are oriented in the 001 crystallographic direction with little periclase occurring interstitially. The loss of MgO is readily apparent by the presence of pores at the grain boundaries of Fig. 22 by comparing with Fig. 23, which represents the fracture surface of an unused brick in which the periclase grains appear to be bonded more tightly.

A fracture surface of the used brick was also examined by the SEM technique. The area in Fig. 24 was obtained at about 8 cm behind the zone of the slag and brick interface and the surface features are almost identical to the surface features of the unused brick in Fig. 23. A SEM micrograph of a fracture surface at the slag and brick interface zone is shown in Fig. 25. In this zone the fracture surface reveals almost total absence of pores, and indicates that the pores are completedly filled by the slag phase.

SLAG CORROSION TESTS

The stability of the direct bonded chrome-magnesia refractories in contact with slag was examined by the cup test technique, in which the materials were reacted for up to 6 hours under high vacuum at 1700°C as opposed to the constantly changing dynamic conditions in the ladle.

A photograph of the cross section of the cups after firing is shown in Fig. 26. The most evident feature is the formation of laminar fissures that have expanded to the point where the adjacent cup wall is slightly distorted. It appears that the laminar fissures are formed along planes of weakness resulting from the gases generated internally and trapped in the slag filled pores. These fissures represent structural weaknesses that would lead to increased wear by erosion/corrosion. A similar feature, but less pronounced, was also found in the altered zone of used ladle bricks.

The microstructure of the cup (Fig. 27) shows that the slag has penetrated throughout the walls and bottom of the cup and silicates have replaced some of the periclase, leaving islands of chrome spinel in a silicate groundmass.

Fig. 28 shows a SEM micrograph of a section of slagged cup. The mineralogy and morphology are similar to the optical micrograph shown in Fig. 27. EDXR maps of the same area for Ca, Si, Al and Fe are given in Fig. 29 to 32 respectively. Both Si and Al are distributed at the grain boundaries of the refractories and outline the channels in which the slag migrated. Both Fe and Al tend to be found mainly in the chrome spinel grains and this suggests that these two elements formed solid solution with the spinel phase.

THERMAL SHOCK AND EXPANSION BEHAVIOUR

Loss of the oxide constitutents from the brick due to volatilization in vacuum leads to weakening of the intergranular bonds of the brick. One would also expect that the cold end of the brick will be more susceptible to failure because of mechanical and thermal stressing which lead to spalling of the hot face. Unused bricks subjected to thermal cycling at 1000°C showed that cracks started to develop after the first cycle. These cracks were further extended and propagated parallel to the hot face after the second cycle. This was in contrast to the used bricks, where the cracks were developed principally after the second thermal cycle. There was no evidence pointing to a symmetrical crack pattern developing with respect to the slag brick interface. However, in the final stages of the test, the cracks were gradually developing a pattern in which they were almost paralled to the slag brick interface. The irregular cracks formed in the unused brick are to be expected since these cracks are likely to follow weaknesses of the microstructure such as the bond characteristic of the spinel and periclase grains. The symmetrical crack pattern observed in the used brick indicates that cracks follow the surface of slag penetration, as this zone suffers greater loss of materials due to vaporization and would have the least strength.

Dynamic thermal expansion tests of the used and unused bricks showed no substantial difference in the amount and rate of expansion between room temperature and 1000°C. Therefore it is unlikely that the brick failure was caused by differential thermal expansion.

POROSITY AND DENSITY OF USED AND UNUSED BRICKS

Both porosity and density of the used and unused bricks were determined and the results are presented in Table 2.

The apparent porosity of the slagged brick and brick at 10 cm behind the slag brick interface falls in the range from 9.7 to 11.4%, compared with 11.3% for the unused brick. The low apparent porosity of the slagged brick indicates that the pores in the brick are impregnated by the slag phase. The density of the used and unused bricks is in the range from 3270 to 3400 kg/m^3.

DISCUSSION

Periclase bonded to periclase is more common in the direct bonded chrome-magnesia brick than in the co-clinkered chrome-magnesia brick. The lack of spinel rimming the periclase grains is not surprising as the brick is less homogenous structurally than the co-clinkered brick. The lack of spinel to spinel bonding in the direct bonded brick makes it more susceptible to slag attack.

Optical and SEM microscopy examination of the used bricks indicate that slag penetration into the brick has caused partial dissolution of the refractories, and also confirm that the slag penetrates mainly along the grain boundaries of the spinel and periclase. The periclase grains are readily dissolved by the slag when in contact. The chrome spinel is more slag resistant and tends to remain almost intact, forming islands in the groundmass of the slag.

The presence of intergranular Ca and Si phase in the direct bonded brick may also have some influence on the failure of the refractories as this phase tends to disrupt the bond of the grains, thus weakening the structure.

In vacuum at high temperature, the behaviour of the direct-bonded brick is similar to that of the co-clinkered brick, which suffered a loss of MgO. The loss of MgO would cause pores to be formed at the grain boundaries, opening up channels for slag to penetrate.

CONCLUSIONS

The bonding characteristics of the direct bonded chrome-magnesia brick is appreciably different from that of the co-clinker chrome-magnesia brick due to differences in fabrication techniques. The lack of uniform distribution of the chrome spinel solid solution, random distribution of the unreacted spinel grains in the periclase and the presence of large periclase grog grains make the direct bonded chrome-magnesia much more susceptible to slag corrosion and erosion than the co-clinkered variety.

Another factor that may cause refractories failure is the loss of MgO in vacuum at high temperature.

ACKNOWLEDGMENTS

The writers wish to express gratitude to the Atlas Steel Company for supplying the necessary materials for this study. Thanks are also due to D.R. Owen for performing the scanning electron microscopic examination, Y. Bourgoin for preparing thin and polished sections for this study, and to G. Lemieux for his assistance in the experimental work.

REFERENCES

1. Chesters, J.H. "Refractories for iron and steelmaking", The Metals Society; ;London; 1974.

2. Spencer, D.R.F. "Development in LD refractories"; Refract J 8-26; 1975.

3. Alcock, S. and Spencer, D.R.F. "The applications and performance of basic refractories in secondary steelmaking ladles"; Trans Br Ceram Soc 77:45-57; 1978.

4. Spencer, D.R.F. "Critical refractory properties and magnesia chrome clinker brick development for AOD application" Refract J Jan-Feb:10-16; 1975.

5. Evens, J.L. "Furnace design and operations - key to refractory performance. Part II. Basic oxygen steelmaking vessels and vacuum degassing"; Refract J Sept-Oct:9-11; 1980.

6. Lakin, J.R. "Assessment techniques in refractories technology" Refract J Nov-Dec:7-10; 1972.

7. Carswell, G.P., Crosby, M.P. and Spencer R.F. "Development of high performance ladle linings"; Refract J Jan-Feb:9-20; 1980.

8. Gittins, D.J., Spencer, D.R.F. and Ball, N. "The application of basic materials in electric arc furnaces"; Refract J Sept-Oct:12-30; 1973.

9. White, J. "An assessment of recent research on refractories (Part One)"; Refract J Nov-Dec:10-19; 1976.

10. Rigby, G.R., Hutton, F.R. and Hamilton, B.G. "Reactions occurring in basic brick"; J Am Ceram Soc 33:121-132; 1963.

11. Berry, T.F., Allen, W.C. and Snow, R.B. "Chemical change in basic brick during service"; J Am Ceram Soc 33:121-132; 1950.

12. Binns, D. "The use of special ceramics in handling molten iron and steel: A review"; Trans Br Ceram Soc 77: 1-12, 1978.

13. Quon, D.H.H. and Bell, K.E. "Degradation of slagline chromemagnesia bricks in secondary steelmaking under vacuum environment: A progress report"; Division Report MRP/MSL 81-83 (IR); CANMET, Energy, Mines and Resources Canada; 1981.

14. Brezny, B. and Schultz, R.L. "Effect of service atmosphere in the structure changes of magnesia-chromite refractories"; Open Hearth Proc 58:121-129; 1975.

15. Orlov, V.A., Sokolov, A.N., Polonskii, Yu.A., Caponov, Ya.G., Mezentsev E.P., Simonov, K.V., Kabonov, V.S., Suvoror, S.A., Kuznetsov, G.I., Chermak A., and Gavlik, V. "New refractories for plants handling the vacuum treatment of steel outside the furnace"; Refractories (Translation from Russion OGNEUPORY) 21:67-80; 1980.

16. Survorov, S.A., Mel'nikov, A.D., Orlov, V.A., Simonov, K.V., Bocharov, L.D., Kuznetsor, G.I., Pereplitsyn, V.A., and Pvinik, L.YA. "Wear of magnesia spinel refractories in production vacuum-processing steel plant"; Refractories (Translated from Russian OGNEUPORY) 21:145-153; 1980.

17. Whiteworth, D.A., Jackson, F.D. and Patrick, R.F. "Fused basic refractories in the argon-oxygen-decarburization process"; Am Ceram Soc Bull 53:804-808; 1974.

18. Furumi, K., Semba, K., and Ono, N. "Wearing mechanism of basic brick at high-temperature in vacuum"; Taikabutsu 31:133-137; 1979.

19. Naoyuki, N., Matsumura, T. and Adachi, H. "Analysis on direct bonded magnesite chromite brick used at slagline of steel ladle"; Taikabutsu 29:8-12; 1977.

Table 1 Compositions of slags used for the cup tests

Slag No. *	Oxides, mass %						CaO/SiO_3 mass ratio
	SiO_2	Cr_2O_3	Al_2O_3	CaO	MgO	Fe_2O_3	
1	33.30	0.63	10.50	44.80	9.81	0.97	1.34
2	38.70	3.98	6.47	41.85	7.10	1.90	1.08
3	38.97	0.67	10.32	35.88	12.69	0.98	0.92
4	38.15	0.43	10.04	36.59	12.79	0.94	0.96
5	33.61	0.49	7.60	39.42	17.85	1.07	1.17
6	37.90	0.80	8.53	39.93	11.80	1.04	1.05

* 1. ladle after teeming final heat.
2. final slag sample after V.O.D. heat.
3. ladle after teeming final heat.
4. final slag sample after V.O.D. heat .
5. ladle after teeming final heat.
6. final slag sample after V.O.D. heat.

Table 2 Porosity of the chrome magnesia bricks

Type	Porosity %	Density
Unused Brick	11.3	3400
Above slag line	11.4	3390
Above slag line, near slag brick interface	12.1	3330
Below slag line	14.0	3270
Below slag line, near slag brick interface	9.78	3390

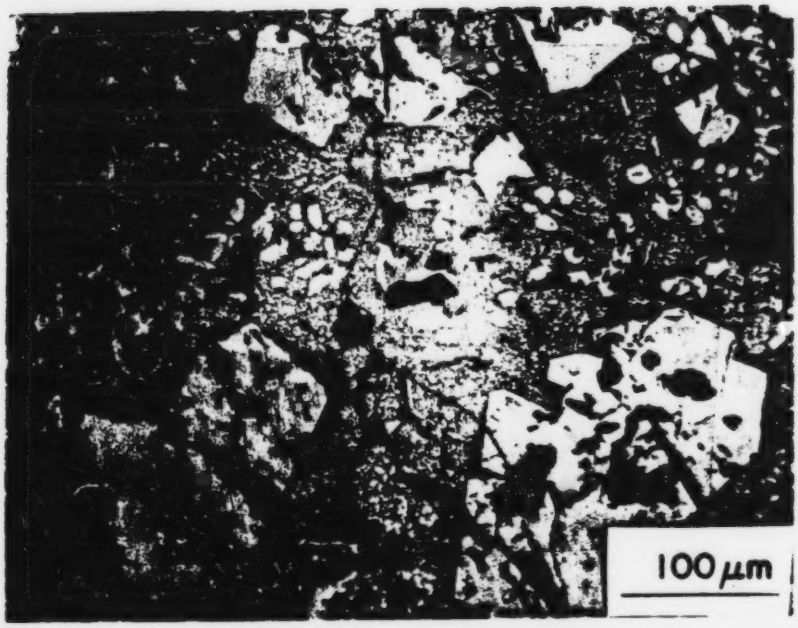

Fig. 1. Typical microstructure of an unused brick

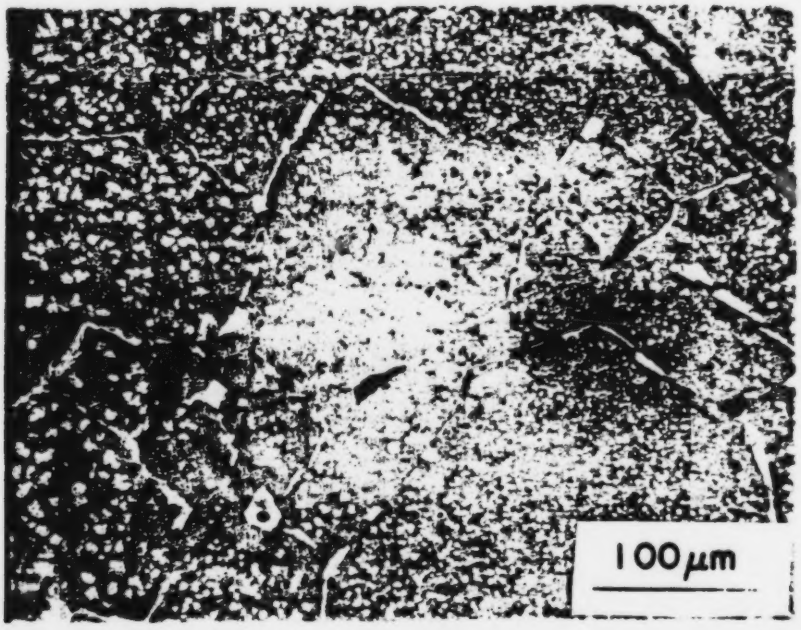

Fig. 2. Photomicrograph showing exsolved spinel phase in and around the periclase grains

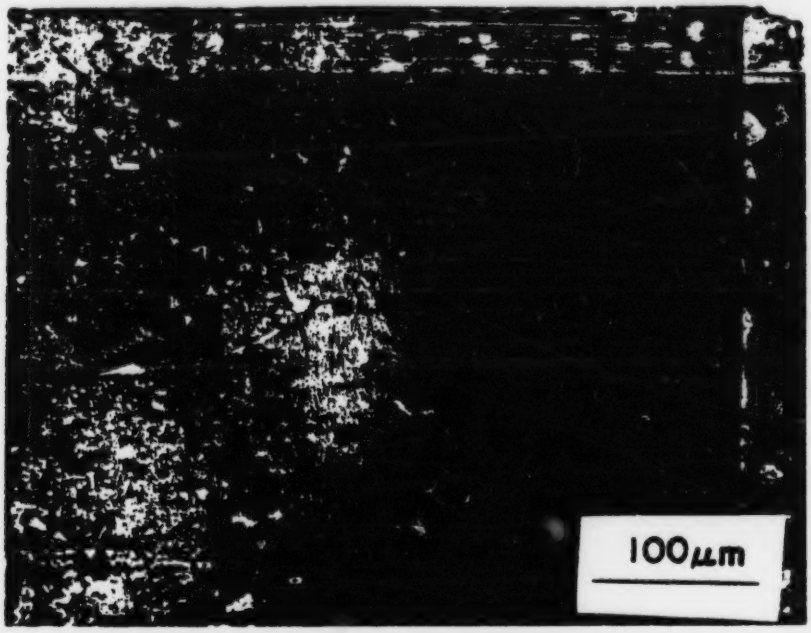

Fig. 3. Micrograph showing coarse grained periclase containing finely exsolved spinel phase

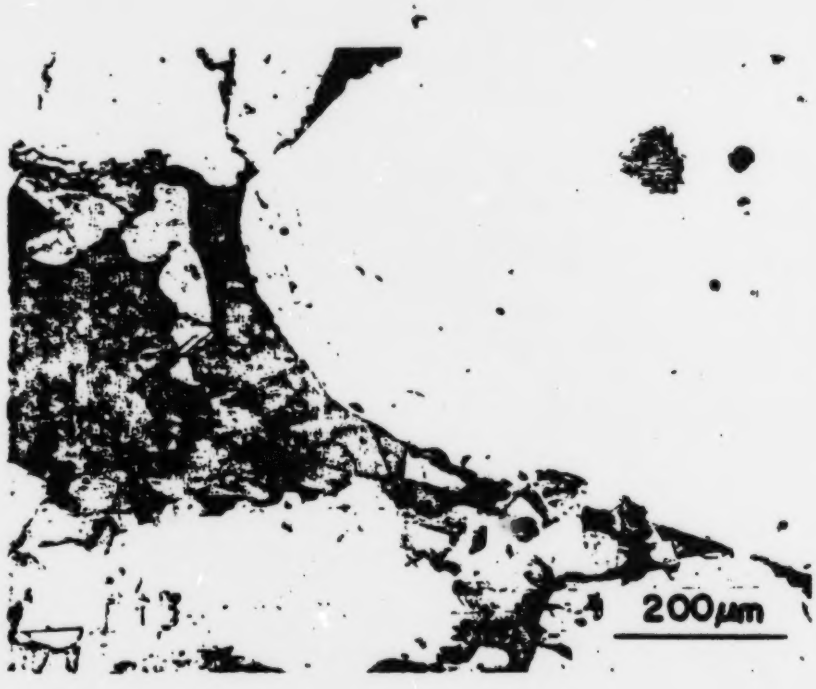

Fig. 4. Micrograph showing coarse grained chrome spinel crystals in a periclase matrix

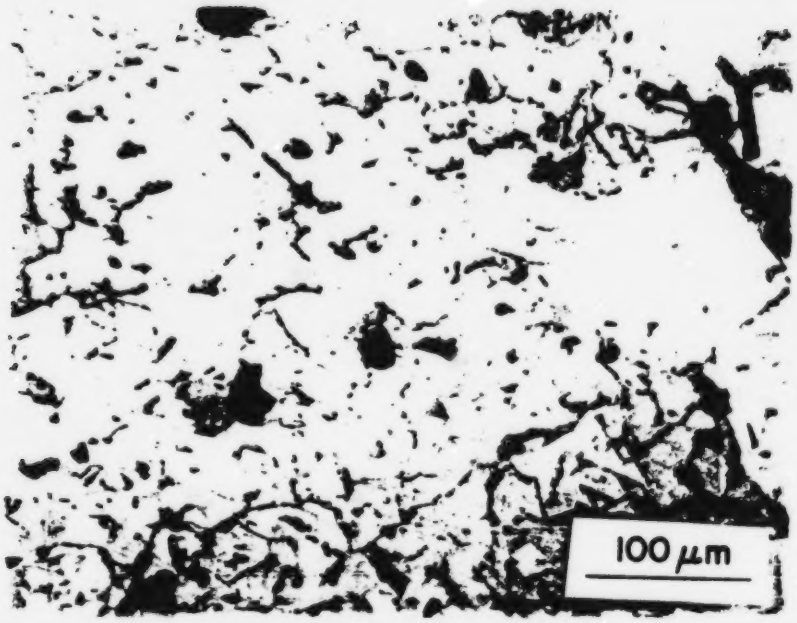

Fig. 5. The skeletal crystals of spinal in a periclase matrix

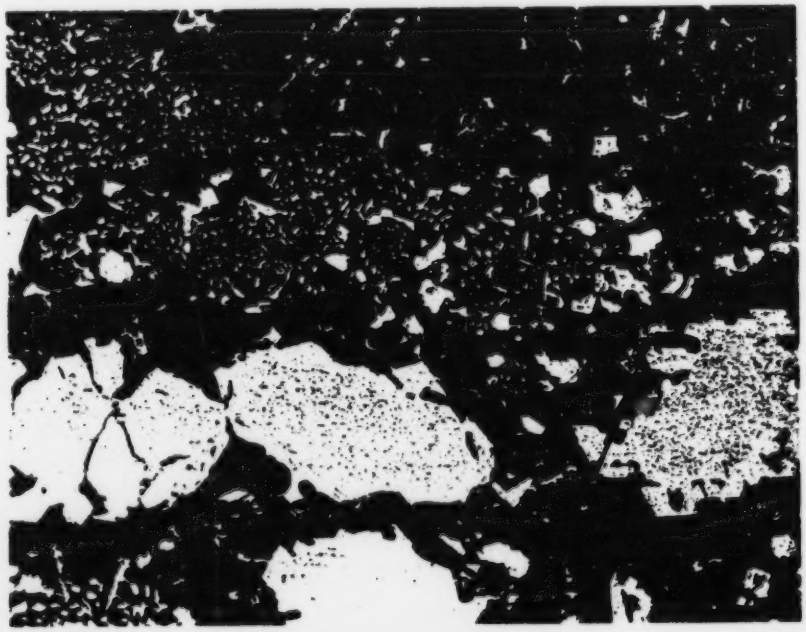

Fig. 6. SEM micrograph of an unused brick

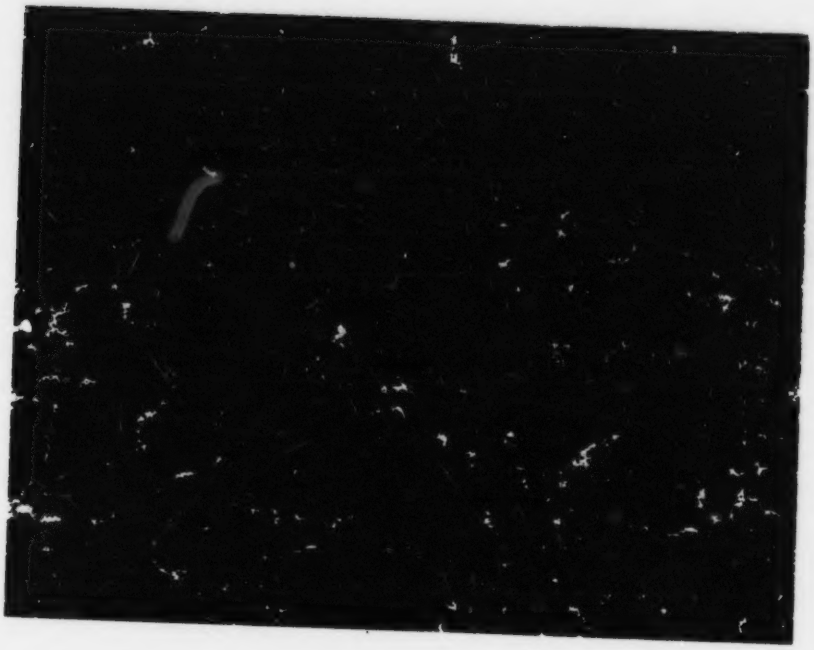

Fig. 7. EDXR map of Ca of an unused brick

Fig. 8. EDXR map of Si of an unused brick

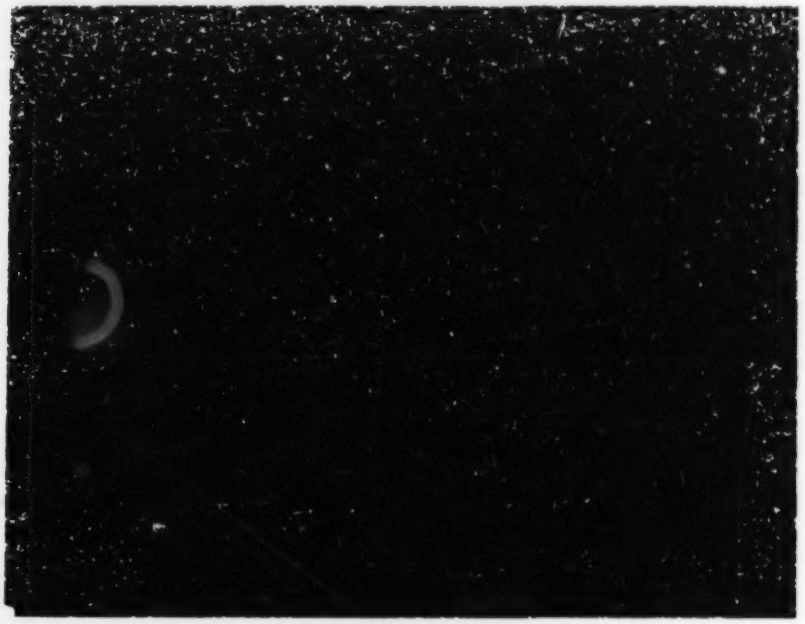

Fig. 9. EDXR map of Fe of an unused brick

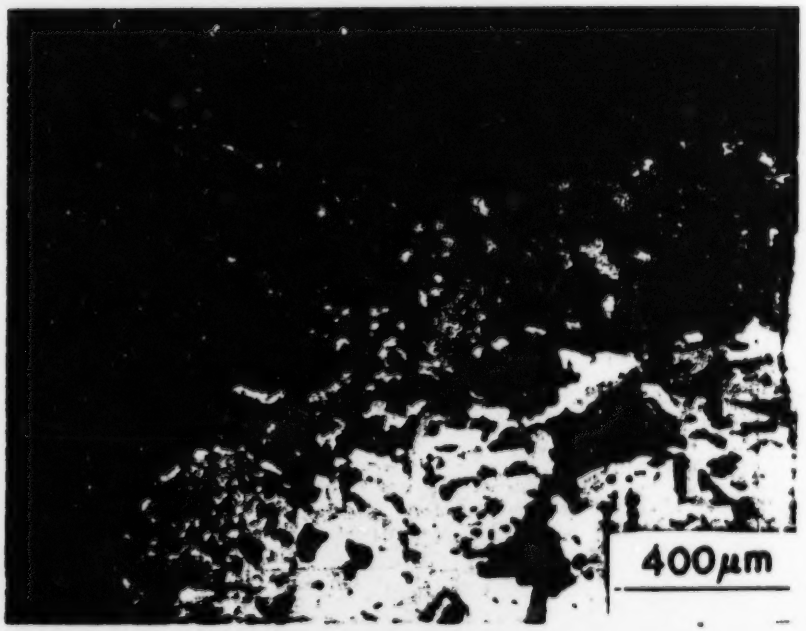

Fig. 10. Microstructure of a used brick at the slag brick interface

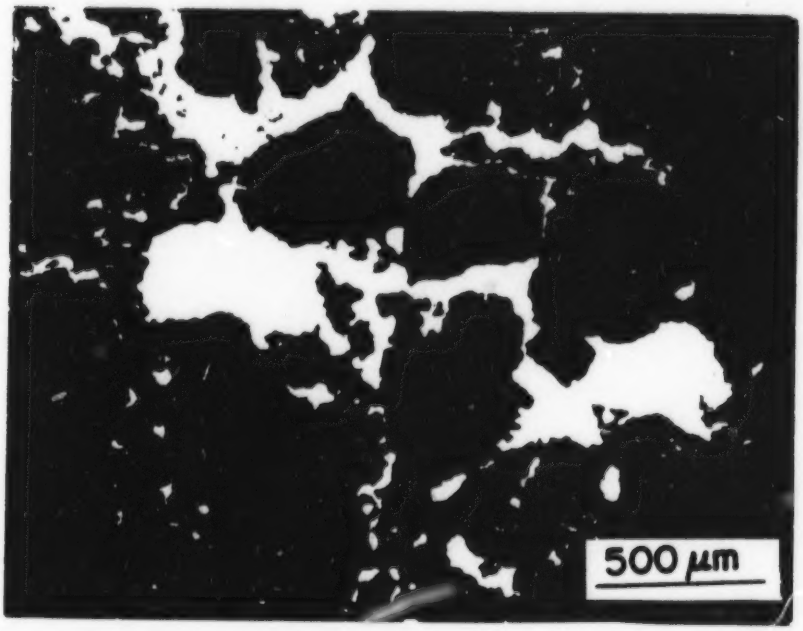

Fig. 11. Microstructure of a used brick viewed under transmitted light

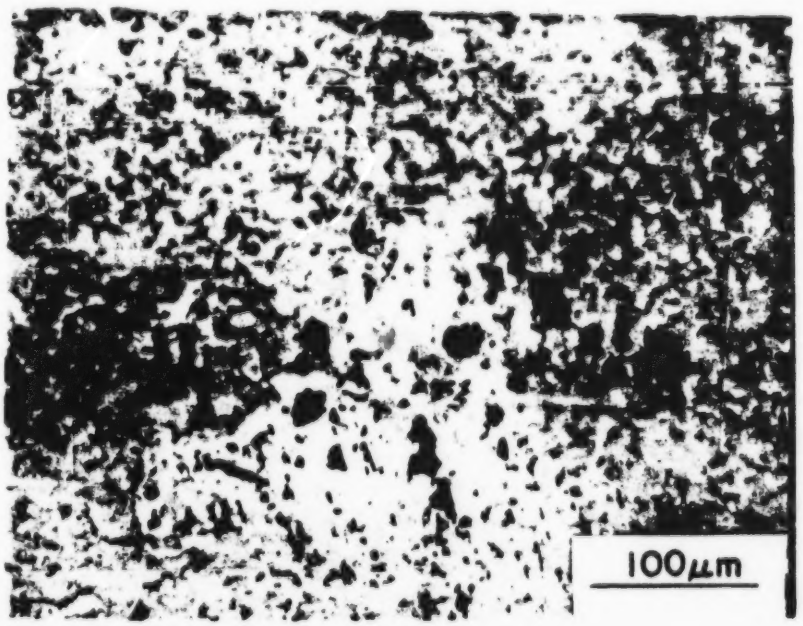

Fig. 12. Microstructure of a used brick showing highly slag resistant spinel phase in a groundmass of slag

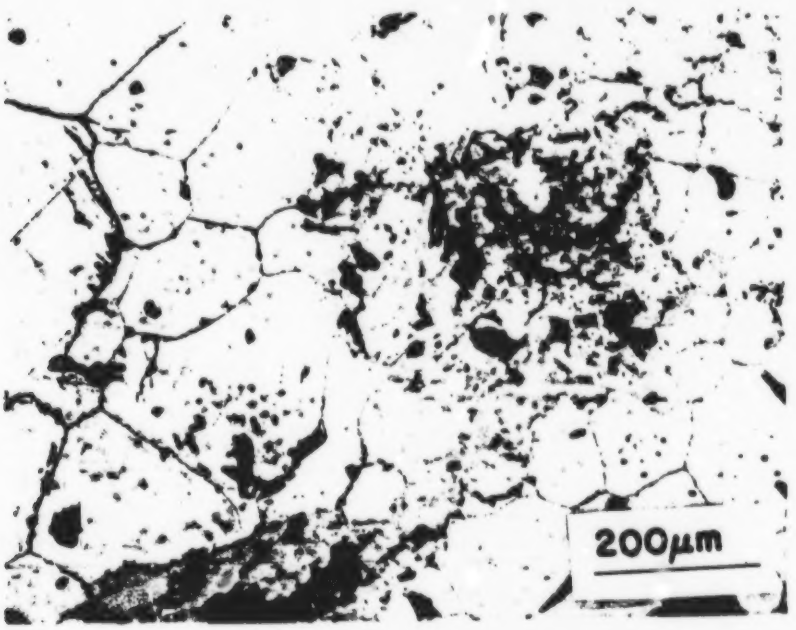

Fig. 13. Microstructure of a used brick showing partial penetration by the slag

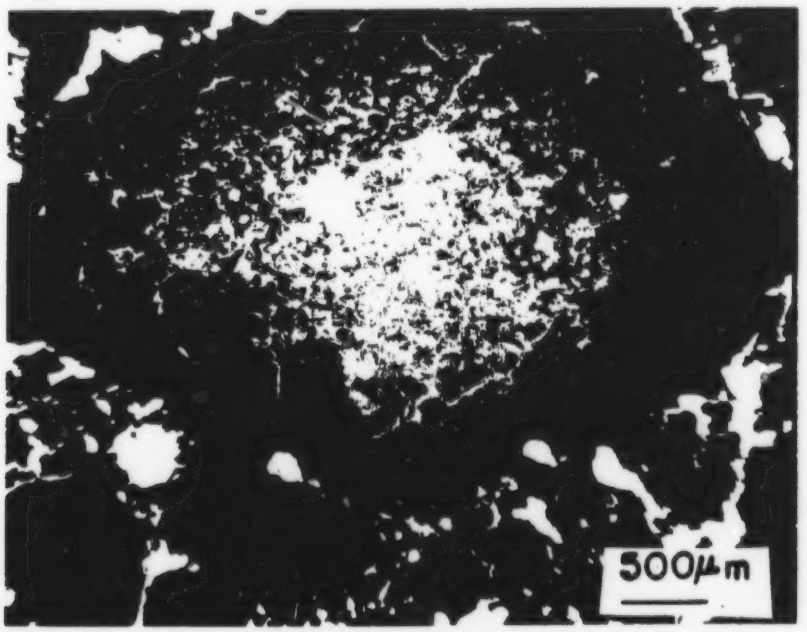

Fig. 14. Micrograph showing slag penetration in the grog grain of periclase and disruption of solid-solid bond of the grains

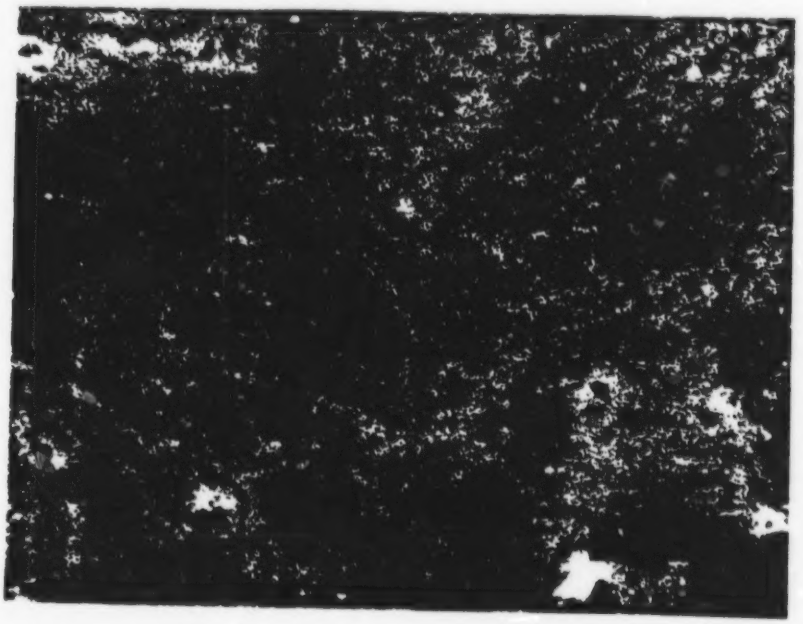

Fig. 15. SEM micrograph of a slagged brick used above the slagline

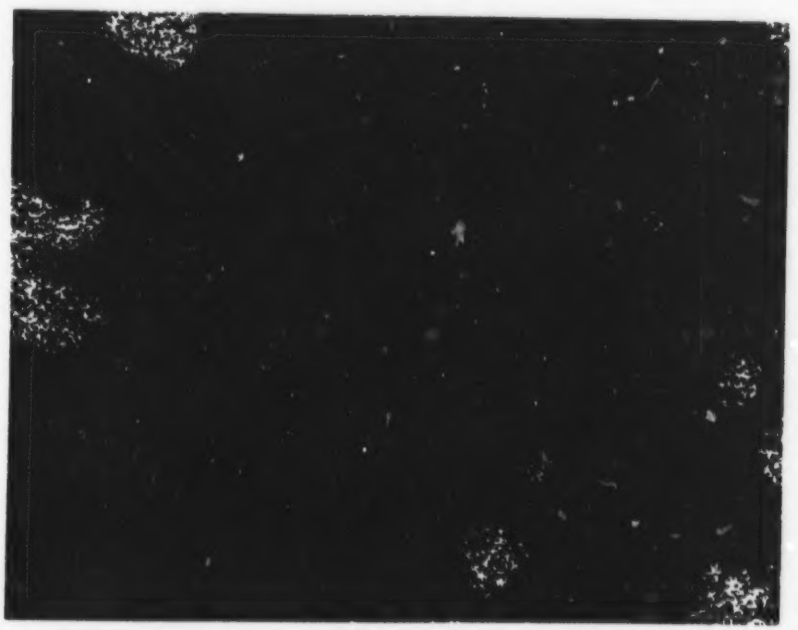

Fig. 16. EDXR map of Mg of a slagged brick

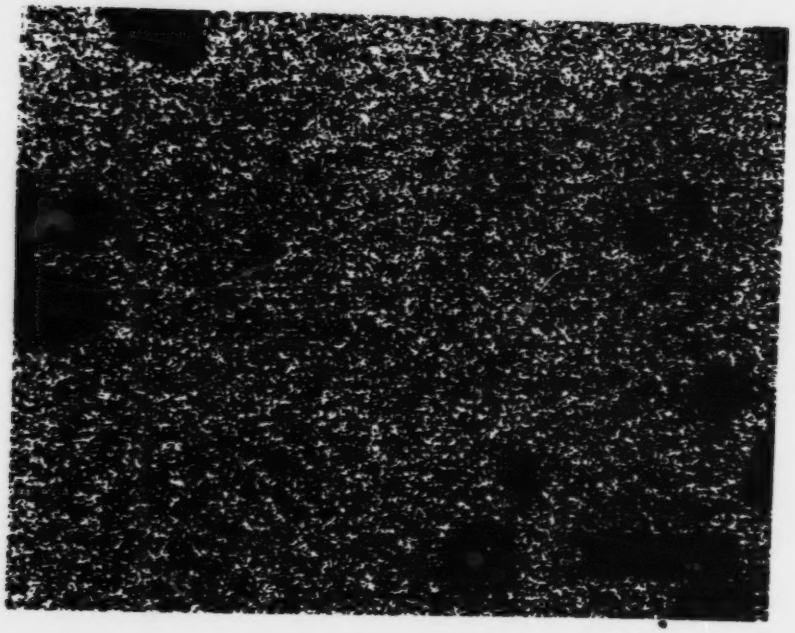

Fig. 17. EDXR map of Ca of a slagged brick

Fig. 18. EDXR map of Si of a slagged brick

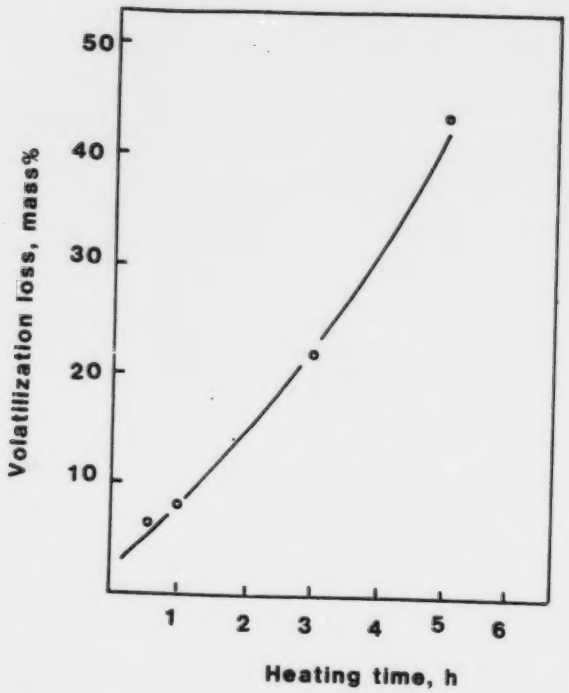

Fig. 19. Vapourization loss versus duration of heating at 1700 C of an unused brick

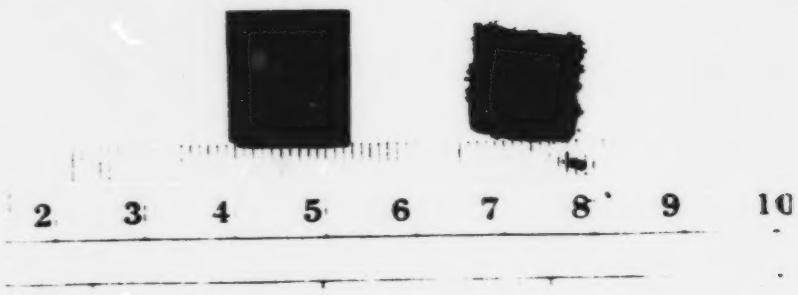

Fig. 20. Photograph showing direct-bonded brick prior to firing (left) and after firing at 1700°C for 5 h (right)

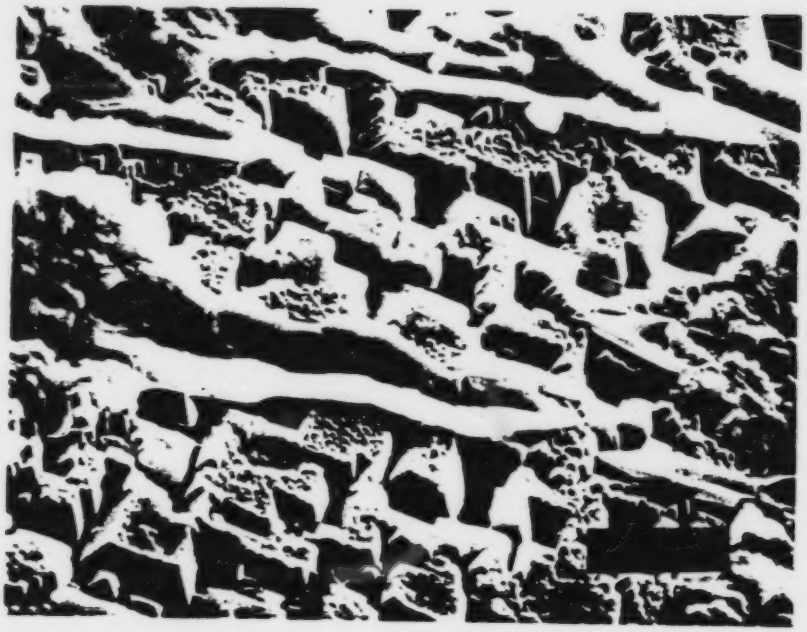

Fig. 21. SEM micrograph of the surface of a brick after firing

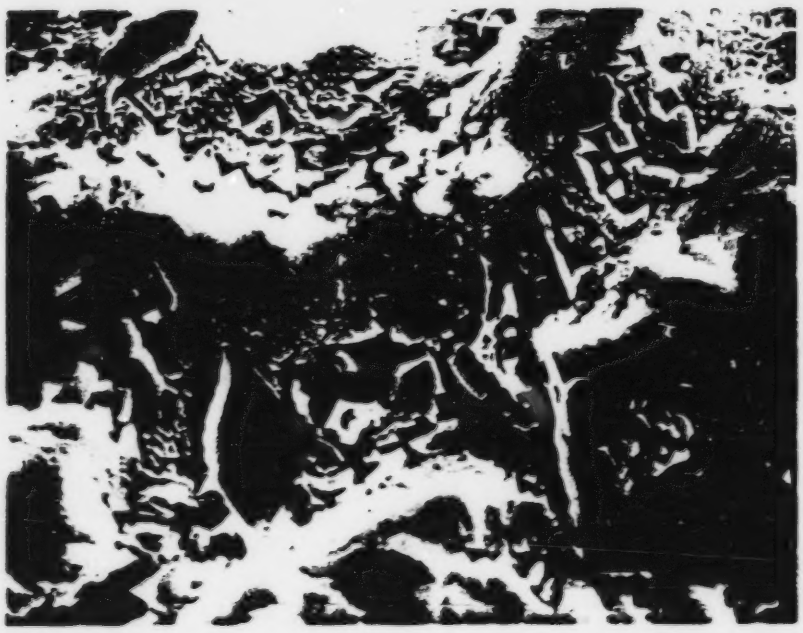

Fig. 22. SEM micrograph of the surface of a brick after firing

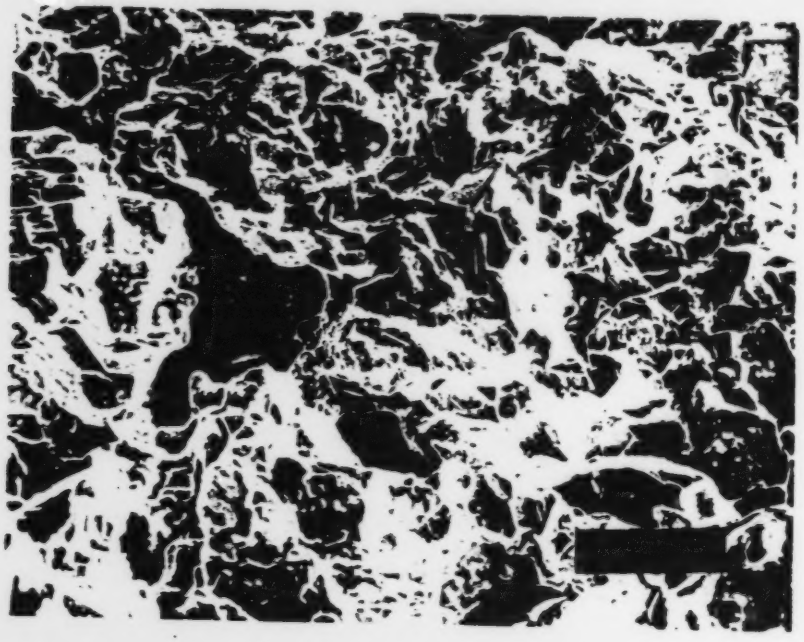

Fig. 23. SEM micrograph of a fracture surface of an unused brick

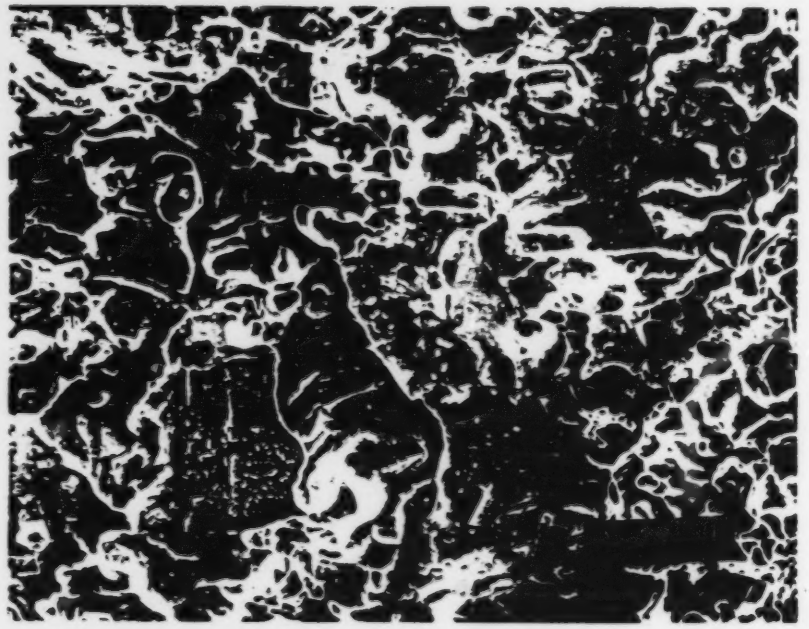

Fig. 24. SEM micrograph of the fracture surface of a used brick at about 8 cm behind the slag brick interface

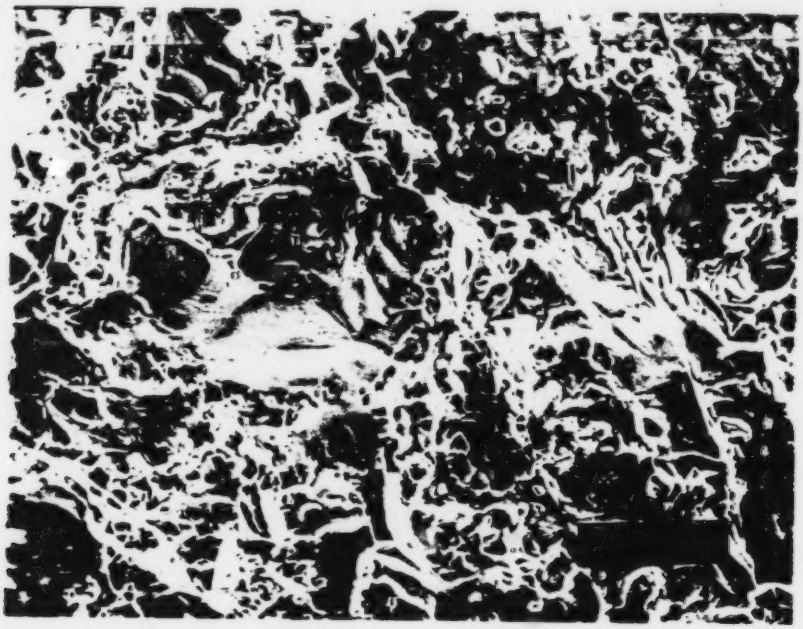

Fig. 25. SEM micrograph of the fracture surface of a slag infiltrated brick

Fig. 26. Section through crucible after slag infiltration

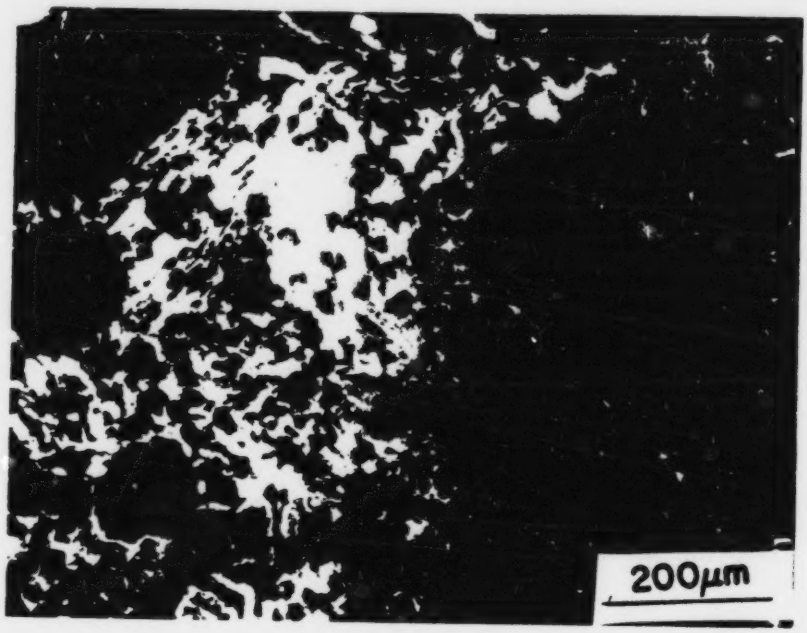

Fig. 27. Micrograph showing lath-shaped silicates formed in slagged brick

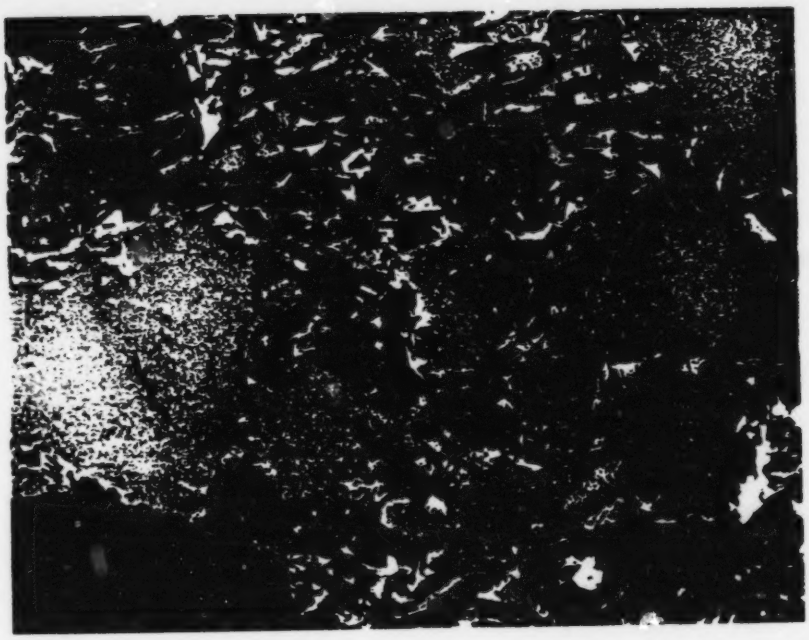

Fig. 28. SEM micrograph showing dissolution of periclase grains by slag

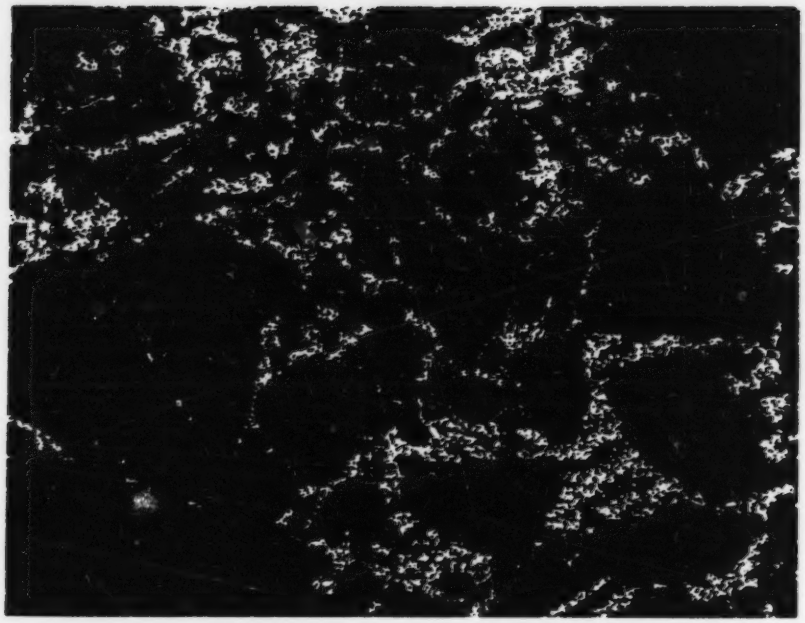

Fig. 29. EDXR map of Ca of a slag corroded crucible

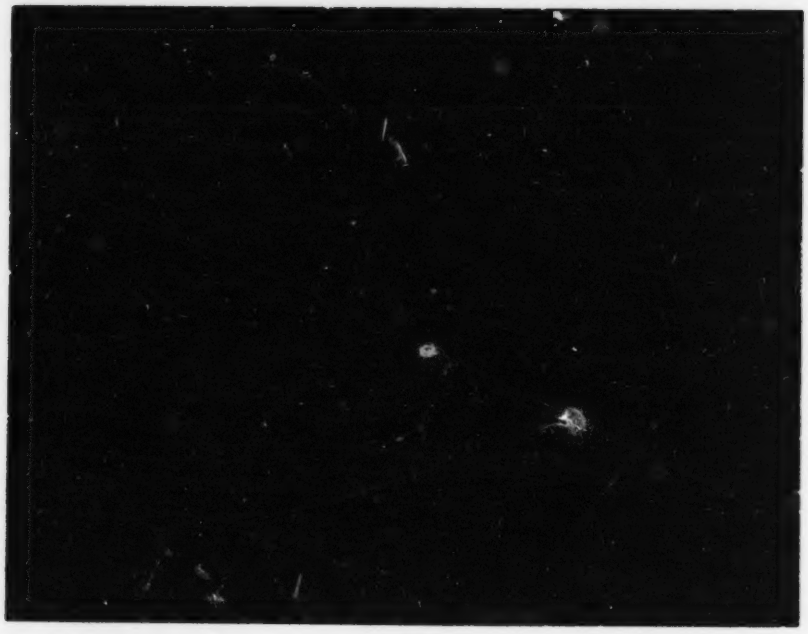

Fig. 30. EDXR map of Si of a slag corroded crucible

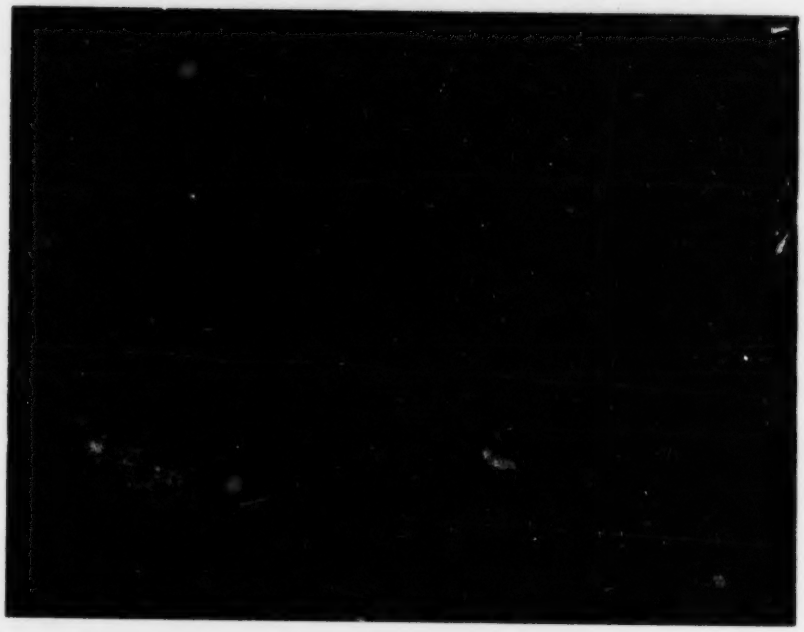

Fig. 31. EDXR map of Al of a slag corroded crucible

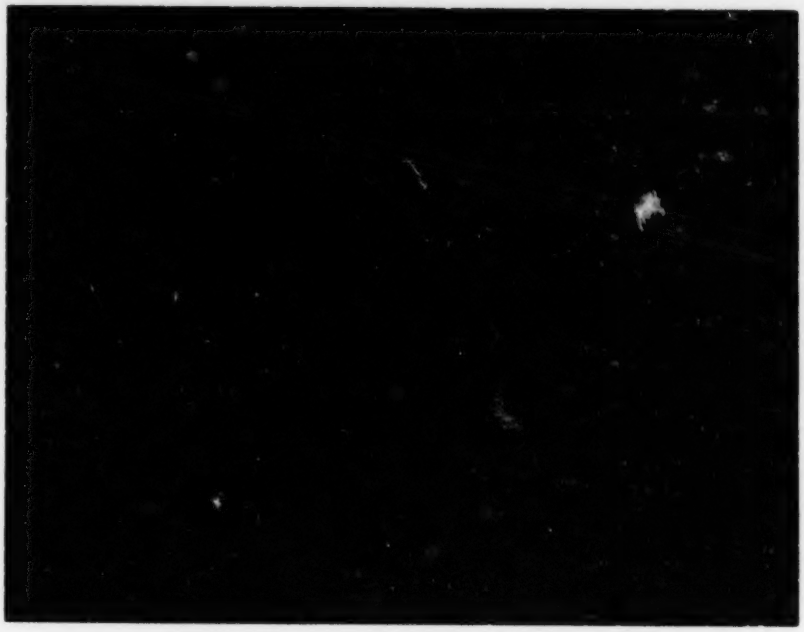

Fig. 32. EDXR map of Fe of a slag corroded crucible